

PAPER • OPEN ACCESS

## Angle-Based Photovoltaic Curve Tracing using Boost Converter

To cite this article: R Ayop *et al* 2021 *J. Phys.: Conf. Ser.* **1878** 012016

View the [article online](#) for updates and enhancements.

You may also like

- [Modeling and analysis of the solar photovoltaic levelized cost of electricity \(LCoE\) - case study in Kupang](#)  
Rusman Sinaga, Nonce F. Tuati, Marthen D.E. Bely et al.
- [An Investigation of the Recovery of Silicon Photovoltaic Cells By Application of an Organic Solvent Method](#)  
Vaidyanathan Subramanian, Prichard Tembo and Milan Heninger
- [Performance of Artificial Neural Network and Particle Swarm Optimization Technique based Maximum Power Point Tracking for Photovoltaic System Under Different Environmental Conditions](#)  
Said Zakaria Said and Lamine Thiaw



## ECS Membership = Connection

**ECS membership connects you to the electrochemical community:**

- Facilitate your research and discovery through ECS meetings which convene scientists from around the world;
- Access professional support through your lifetime career;
- Open up mentorship opportunities across the stages of your career;
- Build relationships that nurture partnership, teamwork—and success!

**Join ECS!**

**Visit [electrochem.org/join](https://electrochem.org/join)**



# Angle-Based Photovoltaic Curve Tracing using Boost Converter

R Ayop<sup>1</sup>, C W Tan<sup>1</sup>, S N Syed Nasir<sup>1</sup>, N M Nordin<sup>1</sup>, M S A Mahmud<sup>1</sup>.

<sup>1</sup>School of Electrical Engineering, Faculty of Engineering, Universiti Teknologi Malaysia, 81310, UTM Johor Bahru, Johor, Malaysia.

Email: razman.ayop@utm.my

**Abstract:** A photovoltaic (PV) curve tracer is equipment that obtains the characteristic curve of the PV that can be used for PV modelling or performance analysis. Currently, the used of the switched-mode power supply in the PV curve tracer application is limited due to the voltage ripple problem. This paper provides the potential and limitation of designing the PV curve tracer using the boost converter. A new angle-based curve tracing algorithm is proposed to produce evenly distributed tracepoints on the PV curve. The PI controller is used to control the boost converter based on the input from the angle-based curve tracing algorithm. The PV curve tracer is simulated using MATLAB/Simulink. The results show that the proposed PV curve tracer is accurate and trace a significant portion of the PV curve.

## 1. Introduction

The photovoltaic (PV) curve tracer is an equipment used to determine the I-V characteristic of the PV. Several parameters are obtained using the PV curve tracer and these parameters are useful especially for the PV modelling. It is also being used to determine the performance of the PV module by comparing the result obtained from the PV curve tracer with the current-voltage (I-V) data from the manufacturer. Although there are various commercial PV curve tracers, this equipment is expensive and limited to a certain input voltage [1].

A simple PV curve tracer uses multiple resistors [2]. Nonetheless, this is not a flexible solution since it involves a high number of resistors and the resistance is fixed at certain values. There is also the use of a capacitor to trace the PV curve [3]. Although the cost of using this method is low, the method requires a suitable capacitance value each time the irradiance changes.

Since the PV tracer is a variable load, several researchers have modified the DC electronic load to the PV curve tracer. The commercial DC electronic load is integrated with the Arduino to allow the commercial DC electronic load to function as the PV curve tracer [4]. There is also the used of the power switch as the DC electronic load as the PV curve tracer [1, 5]. For the DC electronic load, the commonly used power converter is the linear converter [6, 7]. There is also the used combination of passive element and electronic switches in the DC electronic load design [8]. While, the common controller used for the DC electronic load is the proportional-integral controller [6, 8-10]. There is also the used of the fuzzy logic controller in the AC electronic load [9].

Since the switched-mode power supply (SMPS) contain voltage and current ripples, it is hard to produce a precise DC electronic load. As a result, it is not implemented in the PV curve tracer since the voltage ripple may affect the precision of the curve tracing. This paper provides the potential of the boost converter as the PV curve tracer as well as introducing the angle-based curve tracer algorithm. The boost converter is designed for the continuous current mode operation. The proportional-integral (PI)



controller with resistance feedback is used to control the boost controller. The single diode PV model is used to represent a 40 W PV module. The MATLAB/Simulink is used to simulate the proposed PV curve tracer.

## 2. Design of Photovoltaic Curve Tracer

The block diagram of the PV curve tracer is shown in **Figure 1**. The operation starts by sensing the input voltage and current ( $V_i$  and  $I_i$ , respectively). The curve tracing algorithm determines the next step of the operation. To obtain the short or open circuits characteristic of the PV module, the short-open mode,  $M_{so}$ , is produced and send to the short-open circuit. After the short circuit current,  $I_{sc}$ , and open circuit voltage,  $V_{oc}$ , is obtained, the PV curve tracer operates as an electronic load. The reference input resistance,  $R_{i\_ref}$ , is calculated by the curve tracer algorithm and the mode of output resistance,  $M_{Ro}$ , is produced based on the  $R_{i\_ref}$ . Using Ohm's Law, the  $R_i$  is calculated by dividing the  $V_i$  over the  $I_i$ . The  $R_i$  is compared with the  $R_{i\_ref}$  and the different is used by the PI controller to produce the duty cycle,  $D$ . The pulse width modulation, PWM, uses the  $D$  to produce the switching pulse,  $sp$ , and drives the boost converter. The  $D$  is adjusted by the PI controller until the  $R_i$  equals to the  $R_{i\_ref}$ .

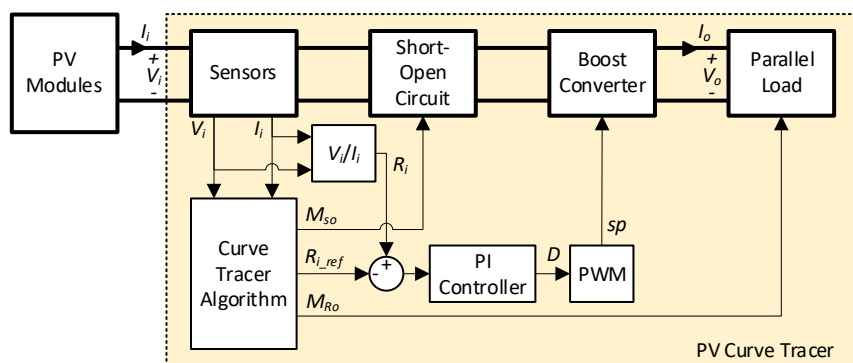


**Figure 1.** The block diagram of the PV curve tracer.

### 2.1. Photovoltaic Model

The standard single diode model is used to test the performance of the PV curve tracer. The PV current,  $I_{pv}$ , is calculated using (1) [11, 12]. Since this equation is an implicit equation, the Newton-Raphson method is used to solve the  $I_{pv}$ . The PV model is based on the Ameresco Solar 40J Photovoltaic Module [13] and the parameters are listed in Table 1.

Table 1: The parameters of the Ameresco Solar 40J Photovoltaic Module [13].

Parameter	Value
Open circuit voltage, $V_{oc}$	22.1 V
Short circuit current, $I_{sc}$	2.32 A
Maximum power voltage, $V_{mp}$	17.9 V
Maximum power current, $I_{mp}$	2.23 A
Temperature coefficient of $I_{sc}$ , $\alpha$	0.105 %/°C
Temperature coefficient of $V_{oc}$ , $\beta$	-0.36 %/°C
Number of cells in series, $N_s$	36

$$I_{pv} = I_{ph} - I_s \left[ \exp \left( \frac{V_{pv} + I_{pv} R_s}{V_t A} \right) - 1 \right] - \frac{V_{pv} + I_{pv} R_s}{R_p} \quad (1)$$

where  $I_{ph}$  is the photo-generated current (A),  $I_s$  is the diode saturated current (A),  $V_{pv}$  is the photovoltaic module voltage (V),  $R_s$  is the series resistance ( $\Omega$ ),  $V_t$  is the junction thermal voltage, where  $V_t = kT/q$ ,  $k$  is the Boltzmann constant ( $1.38 \times 10^{-23}$  J/K),  $T$  is the module temperature (K),  $q$  is the electron charge ( $1.602 \times 10^{-19}$  C),  $A$  is the ideality factor, and  $R_p$  is the parallel resistance ( $\Omega$ ).

## 2.2. Boost Converter

The boost converter is chosen since the  $I_i$  is not disconnected by the switch like the buck and buck-boost converters. This is important in maintaining accurate operation on the I-V characteristic curve of the PV. For the PV curve tracer application, several additional circuits need to be added, as shown in **Figure 1**. At the input of the boost converter, two power switches are added to conduct short and open circuit tests. The parallel load circuit is used as the output of the boost converter. The parallel load is used due to the limitation of the boost converter at the various operating points.

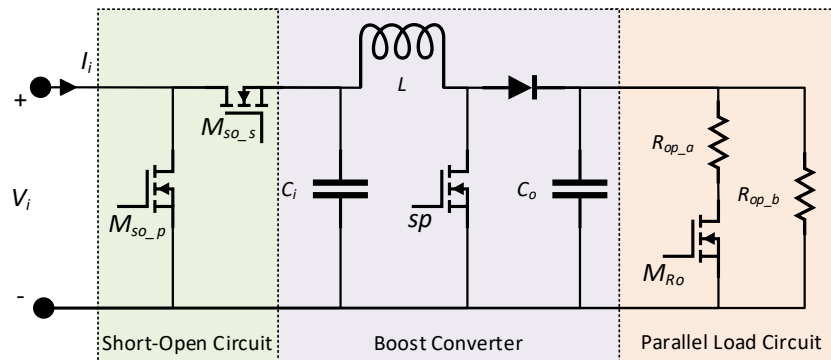


**Figure 1.** The boost converter with the short-open and parallel load circuits.

The implementation of the boost converter for the PV curve tracer application is based on (2) to (6) [14]. It is important to design the boost converter properly since the try and error method may result in the system fail to operate accurately. The first step to design the system is to specify the minimum and maximum duty cycles ( $D_{min}$  and  $D_{max}$ , respectively), as well as the minimum and maximum input resistances ( $R_{i\_min}$  and  $R_{i\_max}$ , respectively), which is calculated using (2). In an ideal condition, the  $R_{i\_min}$  and  $R_{i\_max}$  are zero and infinity, respectively. However, in practice, this cannot be achieved with the boost converter. The  $R_{i\_min}$  and  $R_{i\_max}$  chosen need to cover significant point in the PV curves, which in this case is  $1 \Omega$  to  $80 \Omega$ . The output resistance,  $R_o$ , needs to be calculated properly since the wrong  $R_o$  makes the boost converter operates outside the range of  $D_{min}$  and  $D_{max}$ .

$$R_i = V_i / I_i \quad (2)$$

$$R_{i\_max} / (1 - D_{min})^2 \leq R_o \leq R_{i\_min} / (1 - D_{max})^2 \quad (3)$$

$$L = 4R_o / (27\gamma_{IL}f_s) \quad (4)$$

$$C_i = D / (8L\gamma_{vi}f_s^2) \quad (5)$$

$$C_o = \frac{1}{\gamma_{Vo}f_s} \left[ \frac{1}{R_o} - \sqrt{\frac{R_{i\_min}}{R_o^3}} \right] \quad (6)$$

If the  $R_i$  range of  $1 \Omega$  to  $80 \Omega$  is used in the calculation, the boost converter fails to operate since the  $R_o$  cannot satisfy (3). As a result, two load ranges are needed, as shown in Table 2. This is the reason the parallel circuit load shown in **Figure 1** is needed since a single  $R_o$  unable to satisfied the  $R_i$  range of  $1 \Omega$  to  $80 \Omega$ . The PV curve tracer needs to operate in the continuous current mode operation with the desired voltage ripple. In order to achieve this specification, the inductance ( $L$ ), input capacitance ( $C_i$ ), and output capacitance ( $C_o$ ) are calculated using (4), (5), and (6), respectively and the results are tabulated in Table 2.

**Table 2:** The parameters of the boost converter for two different conditions.

Condition	A	B
Input Resistance, $R_i$	$1 \Omega$ - $12 \Omega$	$12 \Omega$ - $80 \Omega$
Output Resistance, $R_o$	$15 \Omega$	$99 \Omega$
Input Capacitance, $C_i$	$0.2 \mu\text{F}$	$2.2 \mu\text{F}$

Output Capacitance, $C_o$	1.1 $\mu\text{F}$	9.9 $\mu\text{F}$
Inductance, $L$	115.6 $\mu\text{H}$	762.7 $\mu\text{H}$

Based on the parameters for a different condition in Table 2, the maximum values of  $L$ ,  $C_i$ , and  $C_o$  chosen and listed in Table 3. Since the parallel connection of the load is used, the new parallel output resistance,  $R_{op}$ , is calculated using the standard parallel circuit theory.

Table 3: The overall parameters of the boost converter.

Parameter	Value
<b>Desired Specification</b>	
Minimum Duty Cycle, $D_{min}$	10%
Maximum Duty Cycle, $D_{max}$	75%
Switching Frequency, $f_s$	100 kHz
Input Capacitor Ripple Factor, $\gamma_{Ci}$	1%
Output Capacitor Ripple Factor, $\gamma_{Co}$	1%
Inductor Ripple Factor, $\gamma_L$	25%
Safety Factor for $\gamma_{Ci}$	2
Safety Factor for $\gamma_{Co}$	2
Safety Factor for $\gamma_L$	1.3
<b>Calculated Parameters</b>	
Output Resistance, $R_o$	15 $\Omega$ , 80 $\Omega$
Parallel Output Resistance, $R_{op}$	16.3 $\Omega$ , 80 $\Omega$
Input Capacitance, $C_i$ ()	2.2 $\mu\text{F}$
Output Capacitance, $C_o$	9.9 $\mu\text{F}$
Inductance, $L$	762.7 $\mu\text{H}$

The PV curve tracer used the PI controller with the resistance feedback and it is tuned using the try and error method. There is two PI controller used since there are two operating conditions. The proportional and integral gains ( $K_p$  and  $K_i$ ) for the boost converter when  $R_o$  is less than 12  $\Omega$  is 30 and 0.01, respectively. The  $K_p$  and  $K_i$  for the boost converter when  $R_o$  is equal to or more than 12  $\Omega$  is 3 and 0.001, respectively.

### 2.3. Photovoltaic Curve Tracing Algorithm

The PV curve has a non-linear characteristic. As a result, the PV curve tracer cannot change linearly. A linear tracing results in a low number of tracepoints in the constant current region and a high number of tracepoints in the constant voltage region for a high irradiance condition and vice versa. This leads to an inaccurate PV curve tracing. To overcome this problem, the angle-based tracing is introduced to evenly distributed the PV tracepoints using (7) to (12) and the flow chart shown in **Figure 2**.

$$K_{IV} = I_{sc}/V_{oc} \quad (7)$$

$$\theta_{min} = \tan^{-1}(R_{i,min} \times K_{IV}) \quad (8)$$

$$\theta_{max} = \tan^{-1}(R_{i,max} \times K_{IV}) \quad (9)$$

$$\theta_{step} = (\theta_{max} - \theta_{min}) / (N_{res} - 1) \quad (10)$$

$$\theta(i) = \theta_{min} + \theta_{step} \times (i - 1) \quad (11)$$

$$R_i(i) = \tan[\theta(i)] / K_{IV} \quad (12)$$

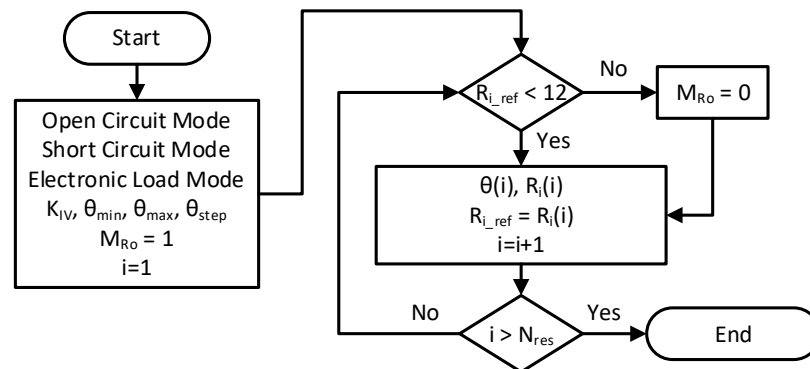


**Figure 2.** The flow chart of the curve tracer algorithm.

The algorithm starts by operating in the open and short circuit modes. In order to operate in this mode, the series and parallel short-open switches ( $M_{so_s}$  and  $M_{so_p}$ , respectively) is controlled based on the switching scheme in Table 4. These modes are operated at the beginning to obtain  $I_{sc}$  and  $V_{oc}$  for the PV curve tracer algorithm. Then, the PV curve tracer operates in the electronic load mode. For the electronic load mode, there are two conditions of operation that depends on the  $R_{i\_ref}$ . If the  $R_{i\_ref}$  is lower than  $12\ \Omega$ , the output resistance switch,  $M_{Ro}$ , is closed  $R_o$  becomes  $15\ \Omega$ . While if the  $R_{i\_ref}$  is  $12\ \Omega$  and above, the  $M_{Ro}$  is open and the  $R_o$  becomes  $80\ \Omega$ . The  $R_{i\_ref}$  is continuously increased according to (12) until the iteration ( $i$ ) is larger than the tracer resolution ( $N_{res}$ ).

Table 4: The switch position for a different mode of operation.

Mode	$M_{so_s}$	$M_{so_p}$	$M_{Ro}$
Open Circuit Mode	0	0	1
Short Circuit Mode	1	0	1
Electronic Load Mode ( $R_{i\_ref} < 12$ )	0	1	1
Electronic Load Mode ( $R_{i\_ref} \geq 12$ )	0	1	0

### 3. Results and Discussions

There are several discussions on the performance of the PV curve tracer. This includes the accuracy, distribution of tracepoints, coverage of tracepoints, and transient performance.

Accuracy is the main aspect when it comes to the PV curve tracer. A good PV curve tracer needs to operate on the I-V curve of the PV. By referring to **Figure 3**, the proposed PV curve tracer able to operate on the I-V curve of the PV model for both  $500\ \text{W/m}^2$  and  $1000\ \text{W/m}^2$ . This shows that the proposed PV curve tracer is accurate.

The evenly distribution tracepoints are also an important aspect when it comes to the PV curve tracing. The proposed PV curve tracer used the angle-based curve tracing algorithm that manipulates the angle in the I-V curve graph. The result in **Figure 3** shows that the tracing points for both  $500\ \text{W/m}^2$  and  $1000\ \text{W/m}^2$  are evenly distributed. By referring to  $14.20\ \text{V}$  for  $500\ \text{W/m}^2$  and  $20.04\ 1000\ \text{W/m}^2$ , there is an uneven gap caused by the switching of load from  $15\ \Omega$  to  $192\ \Omega$ . This results in tracing point move to another location on the I-V curve.

A good PV curve tracer needs to cover the entire curve of the PV. By referring to **Figure 3**, this cannot be achieved using the boost converter. The tracepoints are absent when the  $V_{pv}$  near to zero and  $V_{oc}$ . This is due to the limitation of the boost converter operation. In order to obtain the tracepoints near to zero  $V_{pv}$ , the  $R_i$  needs to be lower than  $1\ \Omega$ . This is achieved by increasing the  $D_{max}$  limit or adding a new parallel load. The boost converter unable to operate properly if the  $D$  is too high, which lead to failing operation of the PV curve tracer. Adding a new parallel load increases the complexity since not only an additional switch is needed, but also another PI controller. To obtain the tracepoints near to  $V_{oc}$ , the  $R_i$  needs to be higher than  $80\ \Omega$ . This is achieved by decreasing the  $D_{min}$  limit or adding a new parallel load. The same effect is observed when the  $D_{min}$  is decreased or adding a new parallel load.

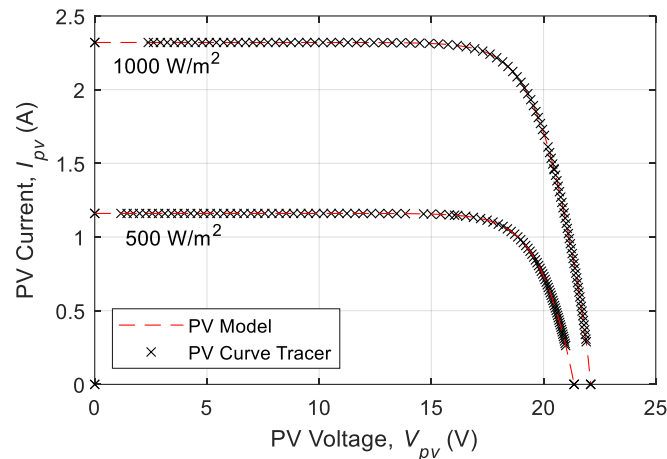


**Figure 3.** The current-voltage (I-V) characteristic curves comparison between the PV model and PV curve tracer at 500 W/m<sup>2</sup> and 1000 W/m<sup>2</sup>.

It is not a common practice to test the transient performance of the PV curve tester [1-5]. Nevertheless, it is an important aspect since the PV module is highly dependent on irradiance that constantly changes. As a result, the I-V curve of a PV module changes with time. If the tracing is not conducted quickly, the I-V characteristic curve changes during the measurement and results in an inaccurate tracing. The transient performance of the PV curve tracer in **Figure 4** shows that the proposed PV curve tracer requires 2.1 s for a complete tracing. The slow transient response is due to the limitation of the boost converter. The boost converter contains inductor and capacitor that slows down the transient response. Reducing the inductance and capacitance in the boost converter improve the transient performance. However, the voltage ripple increases and lead to inaccurate operation of the PV curve tracer. It also results in the boost converter operate in the discontinuous current mode, which requires a different type of closed-loop controller. Reducing the  $N_{res}$  also improve the performance of the PV curve tracer. However, this reduces the number of tracepoints and affect accuracy.

The voltage ripple showed in **Figure 4(a)** is low. This is because the components of the boost converter are designed properly to have the  $\gamma_{Ci}$  at most 1%, which the design used is based on the boost converter with the PV module as the input and not a fixed voltage source. There is also several spikes of  $V_{pv}$  and  $I_{pv}$  observed which caused by the  $R_o$  switching. Nonetheless, the spice does not affect the accuracy of the PV curve tracer.

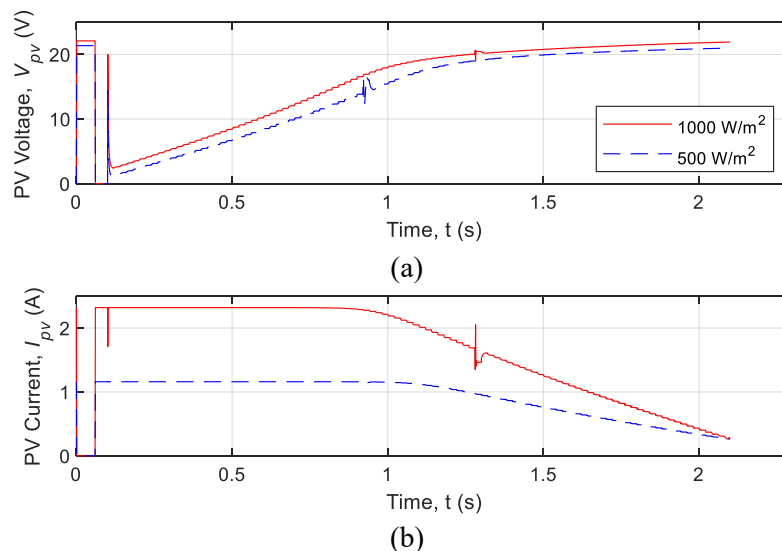


**Figure 4.** The performance of the PV tracer. a) The PV voltage against time. b) The PV current against time.

#### 4. Conclusion

The proposed PV curve tracer able to work properly. The controller was able to trace the PV curve accurately at different irradiance. The angle-based curve tracer algorithm evenly distributed the tracepoints. The voltage ripple produced is low since the boost converter is designed specific to the PV application. Nonetheless, the proposed PV curve tracer unable to fully trace the PV curve due to the limitation of the boost converter. The use of the boost converter also reduces the transient performance of the PV curve tracer. In conclusion, the proposed angle-based curve tracer algorithm able to evenly distribute the tracer points with a minor limitation due to the used of the boost converter in the PV curve tracer.

#### Acknowledgements

The authors would like to express gratitude to Universiti Teknologi Malaysia (UTM) for providing comprehensive library facilities and funding. Funding provided by Universiti Teknologi Malaysia Encouragement Research Grant under vote Q.J130000.2651.18J39. Lastly, thanks to colleagues who have either directly or indirectly contributed to the completion of this work.

#### References

- [1] S. Sarikh, M. Raoufi, A. Bennouna, A. Benlarabi, and B. Ikken, "Implementation of a plug and play I-V curve tracer dedicated to characterization and diagnosis of PV modules under real operating conditions," *Energy Conversion and Management*, vol. 209, p. 112613, 2020/04/01/ 2020.
- [2] A. A. Willoughby, T. V. Omotosho, and A. P. Aizebeokhai, "A simple resistive load I-V curve tracer for monitoring photovoltaic module characteristics," in 2014 5th International Renewable Energy Congress (IREC), 2014, pp. 1-6.
- [3] J. J. M. Ibirriaga, X. M. de Mendiluce Pena, A. Opritescu, D. Sera, and R. Teodorescu, "Low-cost, high flexibility I-V curve tracer for photovoltaic modules," in 2010 12th International Conference on Optimization of Electrical and Electronic Equipment, 2010, pp. 1210-1215.
- [4] P. Papageorgasa, D. Piromalish, T. Valavanisa, S. Kambasisa, T. Iliopouloua, and G. Vokasa, "A low-cost and fast PV IV curve tracer based on an open source platform with M2M communication capabilities for preventive monitoring," *Energy Procedia*, vol. 74, pp. 423-438, 2015.
- [5] N. Saini, A. Mudgal, K. Kumar, J. Srivastava, and V. Dutta, "Design of microcontroller based I-V plotter using IGBT electronic load," in 2016 IEEE 1st International Conference on Power Electronics, Intelligent Control and Energy Systems (ICPEICES), 2016, pp. 1-5.
- [6] K. Lawsri and S. Po-Ngam, "DC electronics load for AH battery testing," in 2017 International Electrical Engineering Congress (iEECON), 2017, pp. 1-4.
- [7] J. Peng, Y. Chen, Y. Fang, and S. Jia, "Design of Programmable DC Electronic Load," in 2016 International Conference on Industrial Informatics - Computing Technology, Intelligent Technology, Industrial Information Integration (ICIIIC), 2016, pp. 351-355.
- [8] A. Shiqi, "High power DC electronic load," in 2017 Chinese Automation Congress (CAC), 2017, pp. 1698-1701.
- [9] E. Mishra and S. Tiwari, "Comparative Analysis of Fuzzy Logic and PI Controller Based Electronic Load Controller for Self-Excited Induction Generator," *Advances in Electrical Engineering*, vol. 2017, p. 5620830, 2017/08/06 2017.
- [10] Z. Meng-Ting, W. Ming-Yan, and W. Le-San, "Design and implementation of a multifunctional DC electronic load," in 2017 IEEE Transportation Electrification Conference and Expo, Asia-Pacific (ITEC Asia-Pacific), 2017, pp. 1-6.
- [11] R. Ayop, C. W. Tan, and C. S. Lim, "The Resistance Comparison Method using Integral Controller for Photovoltaic Emulator," *International Journal of Power Electronics and Drive Systems (IJPEDS)*, vol. 9, 2018.
- [12] R. Ayop and C. W. Tan, "A novel photovoltaic emulator based on current-resistor model using binary search computation," *Solar Energy*, vol. 160, pp. 186-199, 1/15/ 2018.
- [13] A. Solar, "Ameresco Solar 40W Photovoltaic Modules - 40J," ed: Ameresco Inc., 2013.
- [14] R. Ayop and C. W. Tan, "Design of boost converter based on maximum power point resistance for photovoltaic applications," *Solar Energy*, vol. 160, pp. 322-335, 15 January 2018.